Explicit analysis of anisotropic planar waveguides by the analytical transfer-matrix method

Weijun Liao, Xianfeng Chen, Yuping Chen, Yuxing Xia, and Yingli Chen

Department of Physics, The State Key Laboratory on Fiber-Optic Local Area Communication Networks and Advanced Optical Communication Systems, Shanghai Jiao Tong University, 800 Dong Chuan Road, Shanghai 200240, China

The propagation properties of light in anisotropic optical planar waveguides with different index distributions are investigated with the analytical transfer-matrix method. Dispersion equations are analytically deduced by the method in terms of different index profiles. It is shown by examples that this method exhibits good accuracy compared with numerical methods while still holding physical insight. © 2004 Optical Society of America

OCIS codes: 130.2790, 230.7390, 260.1180, 290.3030, 350.5500.

1. INTRODUCTION

As integrated optical components are fabricated with increasingly complicated processes, it becomes more and more essential to analyze the propagation characteristics of optical waveguides with accurate and simple tools. Besides isotropic optical waveguides, anisotropic waveguides have also been widely applied in optical devices. In past decades, some analytical and numerical methods have been presented to solve the propagation characteristics of anisotropic waveguides. Gia Russo and Harris used a ray-approach method[1] to characterize an anisotropic waveguide. A WKB method was proposed by Ctyroky and Cada to analyze inhomogeneous anisotropic planar waveguides.[2] A 4×4 matrix algebra was introduced[3] by Yeh and developed[4] by Visnovsky to investigate light propagation in an arbitrarily anisotropic medium. Kolosovsky *et al.* also proposed a method on the electromagnetic field distribution[5] to characterize anisotropic graded-index slab waveguides with arbitrary parameters. By the method of selecting zero elements in a characteristic matrix,[6] Walpita obtained the solutions for step- and graded-index planar waveguides. Coupled-mode theory was improved by Tsang and Chuang to analyze reciprocal anisotropic waveguides.[7] Additionally, the hybrid modes in planar uniaxial waveguides were calculated based on a rigorous electromagnetic model.[8]

Besides analytical methods, some numerical approaches have been suggested to find the propagation constants of anisotropic waveguides. The finite-element method (FEM) has been well developed for analysis of anisotropic optical waveguides.[9,10] Employing a unique vector potential,[11] the FEM can avoid spurious and nonphysical modes for anisotropic waveguides. The FEM was also adopted to investigate anisotropic waveguides with off-diagonal elements in the permeability tensor[12] and with arbitrary cross sections.[13] In addition to the FEM, the finite-difference time-domain method[14] and the Lanczos–Fourier expansion (LFE) approach[15] were introduced to study asymmetric anisotropic waveguides. A finite-difference (FD) scheme[16] was also used to analyze complicated anisotropic structures of arbitrary index profiles with consideration of the refractive indices in the vicinity of index discontinuities. Furthermore, the surface integral equation method reported by Gaal[17] was used to determine the propagation character of an anisotropic embedded waveguide by minimizing the quadratic difference of the longitudinal field components in the cladding and the core along the dielectric interface. However, the analytical methods can usually obtain only approximate results, while the main deficiency of the numerical methods is a lack of physical insight.

Researchers keep seeking other methods with simplicity, accuracy, and physical insight. Recently, an equivalent attenuation vector (EAV) method based on transfer-matrix analysis was proposed[18] and improved[19] to characterize an isotropic waveguide with good accuracy. In this paper, we begin by analyzing three- and four-layer anisotropic waveguides with an analytical transfer-matrix method, and then we apply an improved EAV method to analyze an anisotropic waveguide with graded-index distribution and discontinuous profile. It is proved by examples that the method can be applied in anisotropic waveguides reliably and accurately.

2. THEORY AND APPLICATIONS

For anisotropic planar waveguides where the principal axes of anisotropy are parallel to the rectangular axes in the coordinate system of the waveguide, as shown in Fig. 1, the dielectric tensor can be depicted in diagonal form as

$$\epsilon = \epsilon_0 \begin{bmatrix} n_x^2 & 0 & 0 \\ 0 & n_y^2 & 0 \\ 0 & 0 & n_z^2 \end{bmatrix}, \tag{1}$$

where ϵ_0 is the permittivity in free space and n_x, n_y, and n_z are the refractive indices of an electric field polarized parallel to the x, y, and z axes of the coordinate system, respectively. In the following analysis, we take the z axis
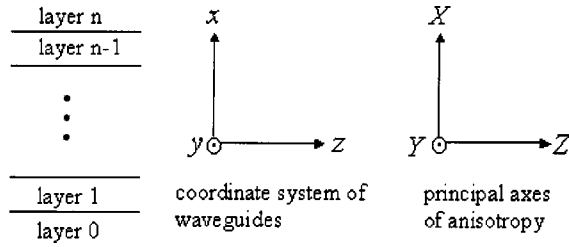
Fig. 1. Principal axes of anisotropy in the coordinate system of a waveguide structure.
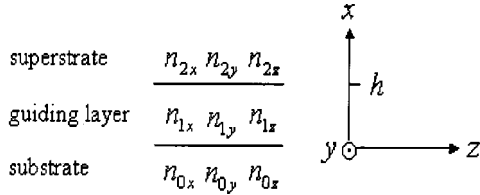
Fig. 2. Coordinate system of a three-layer anisotropic waveguide and index distribution in each layer.

as the propagation direction and assume that the refractive index varies with the x axis and that the waveguide materials are lossless.

A. Three-Layer Anisotropic Waveguide

As shown in Fig. 2, for a three-layer anisotropic waveguide, n_{ix}, n_{iy}, and n_{iz} ($i = 0,1,2$) are the refractive indices of each layer. The thickness of the guiding layer is h, and the superstrate and the substrate are semi-infinite.

The electromagnetic field of a guided wave oscillates in the guiding layer and exponentially attenuates in the superstrate and the substrate. Guided modes in a planar optical waveguide are divided into two types: transverse magnetic (TM) mode and transverse electric (TE) mode, according to the polarization direction of the electromagnetic waves. For the TM mode, the magnetic field can be expressed as

$$H_z(x) = \begin{cases} A_1 \exp(p^{\mathrm{TM}}x), & x \leq 0 \\ B_1 \cos(\kappa_1^{\mathrm{TM}}x) + C_1 \sin(\kappa_1^{\mathrm{TM}}x), & 0 < x < h, \\ D_1 \exp[q^{\mathrm{TM}}(h - x)], & x \geq h \end{cases} \tag{2}$$

where

$$\kappa_1^{\mathrm{TM}} = \frac{n_{1z}}{n_{1x}}(k_0^2 n_{1x}^2 - \beta^2)^{1/2},$$

$$p^{\mathrm{TM}} = \frac{n_{0z}}{n_{0x}}(\beta^2 - k_0^2 n_{0x}^2)^{1/2},$$

$$q^{\mathrm{TM}} = \frac{n_{2z}}{n_{2x}}(\beta^2 - k_0^2 n_{2x}^2)^{1/2},$$

$k_0 = 2\pi/\lambda$, λ is the wavelength in vacuum, and β is the propagation constant for the TM mode.

Based on thin-film theory and the boundary constraints of electromagnetic fields, we can obtain a matrix equation by employing an analytical transfer matrix:

$$\begin{pmatrix} H_z(h) \\ \dfrac{1}{n_{2z}^2} H_z'(h) \end{pmatrix} = \begin{bmatrix} \cos(\kappa_1^{\mathrm{TM}}h) & \dfrac{n_{1z}^2}{\kappa_1^{\mathrm{TM}}} \sin(\kappa_1^{\mathrm{TM}}h) \\[2ex] -\dfrac{\kappa_1^{\mathrm{TM}}}{n_{1z}^2} \sin(\kappa_1^{\mathrm{TM}}h) & \cos(\kappa_1^{\mathrm{TM}}h) \end{bmatrix}$$

$$\times \begin{pmatrix} H_z(0) \\ \dfrac{1}{n_{0z}^2} H_z'(0) \end{pmatrix}. \tag{3}$$

From Eq. (2), we have

$$A_1 \begin{pmatrix} 1 \\ -\dfrac{q^{\mathrm{TM}}}{n_{2z}^2} \end{pmatrix} = \begin{bmatrix} \cos(\kappa_1^{\mathrm{TM}}h) & \dfrac{n_{1z}^2}{\kappa_1^{\mathrm{TM}}} \sin(\kappa_1^{\mathrm{TM}}h) \\[2ex] -\dfrac{\kappa_1^{\mathrm{TM}}}{n_{1z}^2} \sin(\kappa_1^{\mathrm{TM}}h) & \cos(\kappa_1^{\mathrm{TM}}h) \end{bmatrix}$$

$$\times \begin{pmatrix} 1 \\ \dfrac{p^{\mathrm{TM}}}{n_{0z}^2} \end{pmatrix} D_1. \tag{4}$$

Solving the above matrix equation, we can finally get the eigenequation of the three-layer anisotropic waveguide for the TM mode:

$$\tan(\kappa_1^{\mathrm{TM}}h) = \frac{\dfrac{q^{\mathrm{TM}}}{n_{2z}^2} + \dfrac{p^{\mathrm{TM}}}{n_{0z}^2}}{\dfrac{\kappa_1^{\mathrm{TM}}}{n_{1z}^2} - \dfrac{n_{1z}^2}{\kappa_1^{\mathrm{TM}}} \dfrac{q^{\mathrm{TM}}}{n_{2z}^2} \dfrac{p^{\mathrm{TM}}}{n_{0z}^2}}; \tag{5}$$

that is,

$$\kappa_1^{\mathrm{TM}}h = m\pi + \tan^{-1}\left(\frac{n_{1z}^2}{n_{0z}^2} \frac{p^{\mathrm{TM}}}{\kappa_1^{\mathrm{TM}}}\right)$$

$$+ \tan^{-1}\left(\frac{n_{1z}^2}{n_{2z}^2} \frac{q^{\mathrm{TM}}}{\kappa_1^{\mathrm{TM}}}\right) \quad (m = 0,1,2,...). \tag{6}$$

For the TE mode, the electric field can be expressed as

$$E_z(x) = \begin{cases} A_2 \exp(p^{\mathrm{TE}}x), & x \leq 0 \\ B_2 \cos(\kappa_1^{\mathrm{TE}}x) + C_2 \sin(\kappa_1^{\mathrm{TE}}x), & 0 < x < h, \\ D_2 \exp[q^{\mathrm{TE}}(h - x)], & x \geq h \end{cases} \tag{7}$$

where $\kappa_1^{\mathrm{TE}} = (k_0^2 n_{1y}^2 - \beta^2)^{1/2}$, $p^{\mathrm{TE}} = (\beta^2 - k_0^2 n_{0y}^2)^{1/2}$, $q^{\mathrm{TE}} = (\beta^2 - k_0^2 n_{2y}^2)^{1/2}$, and β is the propagation constant for the TE mode. Similarly, we can get the analytical transfer-matrix equation

$$A_2 \begin{pmatrix} 1 \\ -q^{\mathrm{TE}} \end{pmatrix} = \begin{bmatrix} \cos(\kappa_1^{\mathrm{TE}}h) & \dfrac{1}{\kappa_1^{\mathrm{TE}}} \sin(\kappa_1^{\mathrm{TE}}h) \\[2ex] -\kappa_1^{\mathrm{TE}} \sin(\kappa_1^{\mathrm{TE}}h) & \cos(\kappa_1^{\mathrm{TE}}h) \end{bmatrix} \begin{pmatrix} 1 \\ p^{\mathrm{TE}} \end{pmatrix} D_2 \tag{8}$$

and the TE-mode eigenequation

$$\kappa_1^{\text{TE}}h = m\pi + \tan^{-1}\left(\frac{p^{\text{TE}}}{\kappa_1^{\text{TE}}}\right) + \tan^{-1}\left(\frac{q^{\text{TE}}}{\kappa_1^{\text{TE}}}\right)$$

$$(m = 0,1,2,...). \quad (9)$$

Equations (6) and (9) are the well-known result for the guided-mode dispersion equation of the three-layer step anisotropic waveguide for TM and TE modes. By introducing

$$\kappa_1, p, q = \begin{cases} \kappa_1^{\text{TM}}, p^{\text{TM}}, q^{\text{TM}} & \text{for TM mode} \\ \kappa_1^{\text{TE}}, p^{\text{TE}}, q^{\text{TE}} & \text{for TE mode} \end{cases}, \quad (10)$$

$$f_i = \begin{cases} n_{iz}^2 & \text{for TM mode} \\ 1 & \text{for TE mode} \end{cases} \quad (i = 0,1,2), \quad (11)$$

we can finally write the dispersion equation for the three-layer anisotropic waveguide in unified form as

$$\kappa_1 h = m\pi + \tan^{-1}\left(\frac{f_1}{f_0}\frac{p}{\kappa_1}\right) + \tan^{-1}\left(\frac{f_1}{f_2}\frac{q}{\kappa_1}\right)$$

$$(m = 0,1,2,...). \quad (12)$$

B. Four-Layer Anisotropic Waveguide

The mode analysis for a four-layer anisotropic waveguide is given as follows. As shown in Fig. 3, there are two guiding layers. The guided wave may propagate in both guiding layers when the propagation constant β is between $k_0 n_2$ and $k_0 n_3$ or merely in the first guiding layer when β is between $k_0 n_1$ and $k_0 n_2$ while the electromagnetic field in the second layer is evanescent, where n_i ($i = 1,2,3$) is written as n_{ix} for the TM mode and n_{iy} for the TE mode. The two situations will be treated separately in the following discussion.

1. $k_0 n_3 < \beta < k_0 n_2$

Just as in the three-layer case, we can obtain the matrix equation of the four-layer configuration by multiplying analytical transfer matrices in two guiding layers:

$$\left(-\frac{p_0}{f_0} \quad 1\right) M_1 M_2 \left(\begin{array}{c} 1 \\ -\frac{p_3}{f_3} \end{array}\right) = 0, \quad (13)$$

where
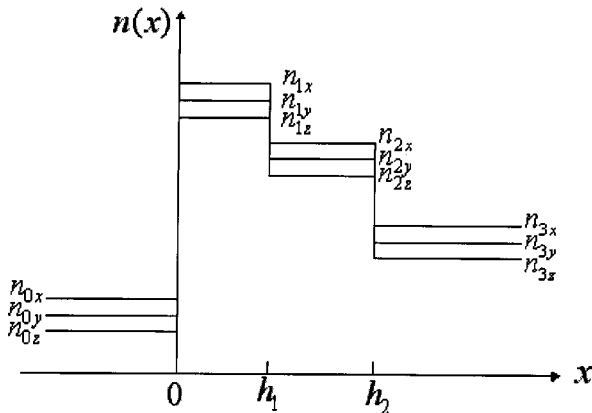
Fig. 3. Index distribution of a four-layer anisotropic waveguide.

$$M_i = \begin{bmatrix} \cos(\kappa_i h_i) & -\frac{f_i}{\kappa_i}\sin(\kappa_i h_i) \\ \frac{\kappa_i}{f_i}\sin(\kappa_i h_i) & \cos(\kappa_i h_i) \end{bmatrix} \quad (i = 1,2),$$

$$\kappa_i = \begin{cases} \kappa_i^{\text{TM}} = \frac{n_{iz}}{n_{ix}}(k_0^2 n_{ix}^2 - \beta^2)^{1/2} & \text{for TM mode} \\ \kappa_i^{\text{TE}} = (k_0^2 n_{iy}^2 - \beta^2)^{1/2} & \text{for TE mode} \end{cases}$$

$$(i = 1,2),$$

$$p_0 = \begin{cases} p_0^{\text{TM}} = \frac{n_{0z}}{n_{0x}}(\beta^2 - k_0^2 n_{0x}^2)^{1/2} & \text{for TM mode} \\ p_0^{\text{TE}} = (\beta^2 - k_0^2 n_{0y}^2)^{1/2} & \text{for TE mode} \end{cases},$$

$$p_3 = \begin{cases} p_3^{\text{TM}} = \frac{n_{3z}}{n_{3x}}(\beta^2 - k_0^2 n_{3x}^2)^{1/2} & \text{for TM mode} \\ p_3^{\text{TE}} = (\beta^2 - k_0^2 n_{3y}^2)^{1/2} & \text{for TE mode} \end{cases},$$

$$f_i = \begin{cases} n_{iz}^2 & \text{for TM mode} \\ 1 & \text{for TE mode} \end{cases} \quad (i = 0,1,2,3).$$

The form of M_i is the so-called oscillatory analytical transfer matrix. Similarly, we get the eigenvalue equation of the four-layer anisotropic waveguide:

$$\kappa_1 h_1 = m\pi + \tan^{-1}\left(\frac{f_1}{f_0}\frac{p_0}{\kappa_1}\right) + \tan^{-1}\left(\frac{f_1}{f_2}\frac{p_2}{\kappa_1}\right)$$

$$(m = 0,1,2,...), \quad (14)$$

where p_2 is obtained by multiplying M_2 and $\left(\begin{array}{c} 1 \\ -p_3/f_3 \end{array}\right)$. After some algebraic transformation and employing

$$p_2 = \kappa_2 \tan\left[\tan^{-1}\left(\frac{f_2}{f_3}\frac{p_3}{\kappa_2}\right) - \kappa_2 h_2\right], \quad (15)$$

we can rewrite Eq. (15) as

$$\kappa_2 h_2 + \Phi_2 = m'\pi + \tan^{-1}\left(\frac{f_2}{f_3}\frac{p_3}{\kappa_2}\right) \quad (m' = 0,1,2,...),$$

$$(16)$$

where $\Phi_2 = \tan^{-1}(p_2/\kappa_2)$. Adding the left- and right-hand sides part of Eqs. (14) and (16) gives the eigenvalue equation of the four-layer anisotropic optical waveguide:

$$\kappa_1 h_1 + \kappa_2 h_2 + \Phi(s)$$

$$= m\pi + \tan^{-1}\left(\frac{f_1}{f_0}\frac{p_0}{\kappa_1}\right) + \tan^{-1}\left(\frac{f_2}{f_3}\frac{p_3}{\kappa_2}\right)$$

$$(m = 0,1,2,...), \quad (17)$$

where $\Phi(s) = \Phi_2 - \tan^{-1}[(f_1/f_2)(\kappa_2/\kappa_1)\tan \Phi_2]$.

2. $k_0 n_2 < \beta < k_0 n_1$

The electromagnetic wave is evanescent in the second layer when β is between $k_0 n_1$ and $k_0 n_2$; then $\kappa_2 = i\alpha_2$, where α_2 is equal to $(n_{2z}/n_{2x})(\beta^2 - k_0^2 n_{2x}^2)^{1/2}$ for the TM mode or $(\beta^2 - k_0^2 n_{2y}^2)^{1/2}$ for the TE mode. Based on the mathematical relations $\sin(ix) = i\sinh(x)$ and $\cos(ix) = \cosh(x)$, the analytical transfer matrix in the second layer in the evanescent case is

$$M_2 = \begin{bmatrix} \cosh(\alpha_2 h_2) & -\dfrac{f_2}{\alpha_2}\sinh(\alpha_2 h_2) \\[2ex] -\dfrac{\alpha_2}{f_2}\sinh(\alpha_2 h_2) & \cosh(\alpha_2 h_2) \end{bmatrix}.$$

Here the form of M_2 is called an evanescent analytical transfer matrix. Similarly, p_2 is expressed as $p_2 = \alpha_2 \tanh\{\tanh^{-1}[(f_2/f_3)(p_3/\alpha_2)] + \alpha_2 h_2\}$.

Finally, the eigenvalue equation in such a situation is rectified as

$$\kappa_1 h = m\pi + \tan^{-1}\left(\frac{f_1}{f_0}\frac{p_0}{\kappa_1}\right) + \tanh^{-1}\left(\frac{f_1}{f_2}\frac{p_2}{\kappa_1}\right)$$

$$(m = 0,1,2,...). \quad (18)$$

C. Graded-Index Anisotropic Waveguide

In Subsections 2.A and 2.B, the guided-mode equation in step three- and four-layer anisotropic waveguides has been investigated by an analytical transfer-matrix method. The graded-index waveguide can be regarded as a step multilayer waveguide if we divide the graded-index profile into numerous step layers. In the following, we employ the analytical transfer-matrix method in the case of an anisotropic waveguide by introducing the improved EAV concept. The improved analysis adopts an EAV to characterize the evanescent field beyond the turning point. Unlike WKB analysis, this method establishes that the phase loss at a turning point is exactly equal to π, independent of the wavelength, the propagation constant, and the refractive-index profile, which is also proved in the quantization condition.[20]

For a graded-index anisotropic waveguide, we take the refractive-index profile as the following arbitrary form, shown in Fig. 4:

$$n_x(x) = \begin{cases} n_{sx} + \Delta n_x f_1(x/D_1), & x \geq 0 \\ n_{cx}, & x < 0 \end{cases}$$

$$n_y(x) = \begin{cases} n_{sy} + \Delta n_y f_2(x/D_2), & x \geq 0 \\ n_{cy}, & x < 0 \end{cases}$$

$$n_z(x) = \begin{cases} n_{sz} + \Delta n_z f_3(x/D_3), & x \geq 0 \\ n_{cz}, & x < 0 \end{cases}$$

where n_{sx}, n_{sy}, n_{sz} and n_{cx}, n_{cy}, n_{cz} are the refractive indices of the substrate and the cover, respectively, Δn_x, Δn_y, and Δn_z are index modulations, and $f_1(x/D_1)$, $f_2(x/D_2)$, and $f_3(x/D_3)$ are index profile functions. As a practical example, this kind of index profile can be found in an annealed proton-exchanged (APE) waveguide or a Ti-diffused waveguide in lithium niobate.

x_t is assumed as the turning point, and then the propagation constant β can be calculated as $\beta = k_0 n_x(x_t)$ (for the TM mode) or $\beta = k_0 n_y(x_t)$ (for the TE mode). Furthermore, we assume that x_s is close enough to the substrate that $n_x(x_s)$ and $n_y(x_s)$ are equal to n_{sx} and n_{sy}, respectively. There are l divided layers from x_0 to x_t and m divided layers from x_t to x_s with uniform thickness h and constant refractive indices $n_x(x_i)$, $n_y(x_i)$, and $n_z(x_i)$ for each layer, as shown in Fig. 4.

Fig. 4. Graded-index anisotropic waveguide with arbitrary index profile.

It is known that the electromagnetic wave has an exponential convergence in the superstrate ($x < 0$) and an oscillatory behavior in the guiding area from x_0 to x_t, where every divided piece can be characterized by an oscillatory analytical transfer matrix. The electromagnetic field is evanescent from x_t to x_s, where each divided slice can be characterized by an evanescent analytical transfer matrix.

According to transfer-matrix theory, we obtain the matrix equation

$$\left(-\frac{p_c}{f_c} \quad 1\right)\left(\prod_{i=1}^{l} M_i\right)\left(\prod_{j=l+1}^{l+m} M_j\right)\left(\begin{array}{c} 1 \\ -\dfrac{p_s}{f_s} \end{array}\right) = 0, \quad (19)$$

where

$$M_i = \begin{bmatrix} \cos(\kappa_i h) & -\dfrac{f_i}{\kappa_i}\sin(\kappa_i h) \\[2ex] \dfrac{\kappa_i}{f_i}\sin(\kappa_i h) & \cos(\kappa_i h) \end{bmatrix} \quad (i = 0,1,2,...,l),$$

$$M_j = \begin{bmatrix} \cosh(\alpha_j h) & -\dfrac{f_i}{\alpha_j}\sinh(\alpha_j h) \\[2ex] -\dfrac{\alpha_j}{f_j}\sinh(\alpha_j h) & \cosh(\alpha_j h) \end{bmatrix}$$

$$(j = l+1, l+2,...,l+m),$$

with

$$\kappa_i = \begin{cases} \kappa_i^{\mathrm{TM}} = \dfrac{n_{iz}}{n_{ix}}(k_0^2 n_{ix}^2 - \beta^2)^{1/2} & \text{for TM mode} \\[2ex] \kappa_i^{\mathrm{TE}} = (k_0^2 n_{iy}^2 - \beta^2)^{1/2} & \text{for TE mode} \end{cases}$$

$$(i = 0,1,2,...,l),$$

$$\alpha_j = \begin{cases} \alpha_i^{\mathrm{TM}} = \dfrac{n_{jz}}{n_{jx}}(\beta^2 - k_0^2 n_{jx}^2)^{1/2} & \text{for TM mode} \\[2ex] \alpha_i^{\mathrm{TE}} = (\beta^2 - k_0^2 n_{jy}^2)^{1/2} & \text{for TE mode} \end{cases}$$

$$(j = l+1, l+2,...,l+m),$$

$$p_c = \begin{cases} p_c^{\text{TM}} = \dfrac{n_{cz}}{n_{cx}}(\beta^2 - k_0^2 n_{cx}^2)^{1/2} & \text{for TM mode} \\[2mm] p_c^{\text{TE}} = (\beta^2 - k_0^2 n_{cy}^2)^{1/2} & \text{for TE mode} \end{cases},$$

$$p_s = \begin{cases} p_s^{\text{TM}} = \dfrac{n_{sz}}{n_{sx}}(\beta^2 - k_0^2 n_{sx}^2)^{1/2} & \text{for TM mode} \\[2mm] p_s^{\text{TE}} = (\beta^2 - k_0^2 n_{sy}^2)^{1/2} & \text{for TE mode} \end{cases},$$

$$f_k, f_c, f_s = \begin{cases} n_{kz}^2, n_{cz}^2, n_{sz}^2 & \text{for TM mode} \\ 1 & \text{for TE mode} \end{cases}$$

$$(k = 0,1,2,...,l + m).$$

Now the EAV p_t is used to describe the evanescent field from the turning point to the substrate, and Eq. (19) becomes

$$\left(-\frac{p_c}{f_c} \quad 1\right)\left(\prod_{i=1}^{l} M_i\right)\begin{pmatrix} 1 \\ -\dfrac{p_t}{f(x_t)} \end{pmatrix} = 0. \tag{20}$$

p_t is determined by the following iterative equations:

$$p_t = p_{l+1},$$

$$p_j = \alpha_j \frac{\dfrac{p_{j+1}}{\alpha_j}\dfrac{f_j}{f_{j+1}} + \tanh(\alpha_j h)}{1 + \dfrac{p_{j+1}}{\alpha_j}\dfrac{f_j}{f_{j+1}}\tanh(\alpha_j h)}$$

$$p_{l+m+1} = p_s, \qquad (j = l + 1, l + 2,...,l + m), \tag{21}$$

Similar to the conclusion for the four-layer anisotropic waveguide in Subsection 2.B, we can obtain the following dispersion equation for a graded-index profile:

$$\sum_{i=0}^{l} \kappa_i h + \Phi_s = N\pi + \tan^{-1}\left(\frac{f_0}{f_c}\frac{p_c}{\kappa_0}\right) + \tan^{-1}\left[\frac{f(x_t)}{f_{l+1}}\frac{p_t}{\kappa_t}\right]$$

$$(N = 0,1,2,...). \tag{22}$$

Because $\kappa_t = 0$ and $\tan^{-1}\{[f(x_t)/f_{l+1}](p_t/\kappa_t)\} = \pi/2$, Eq. (22) can be further written as

$$\sum_{i=0}^{l} \kappa_i h + \Phi_s = N\pi + \tan^{-1}\left(\frac{f_0}{f_c}\frac{p_c}{\kappa_0}\right) + \frac{\pi}{2}, \tag{23}$$

where

$$\Phi_s = \sum_{i=0}^{l-1}\left\{\Phi_{i+1} - \tan^{-1}\left[\frac{f_i}{f_{i+1}}\frac{\kappa_{i+1}}{\kappa_i}\tan(\Phi_{i+1})\right]\right\}, \tag{24}$$

$$\Phi_i = \tan^{-1}\left(\frac{p_i}{\kappa_i}\right), \tag{25}$$

$$p_i = \kappa_i \tan\left[\tan^{-1}\left(\frac{f_i}{f_{i+1}}\frac{p_{i+1}}{\kappa_i}\right) - \kappa_i h\right]$$

$$(i = 1,2,...,l). \tag{26}$$

Furthermore, when the second-order minor term is neglected, Eqs. (24) and (26) can be rewritten as

$$\Phi_s = \sum_{i=0}^{l-1}\frac{p_{i+1}f_{i+1}}{p_{i+1}^2 + \kappa_{i+1}^2}$$

$$\times (\kappa_i/f_i - \kappa_{i+1}/f_{i+1}), \tag{27}$$

$$\frac{p_{i+1}/f_{i+1} - p_i/f_i}{h} = \frac{p_i^2 + \kappa_i^2}{f_i^2}. \tag{28}$$

When the divided layers are infinitely increased, the thickness h of each layer will approach zero. According to the theory of integration and differential calculus, $\Sigma_{i=0}^{l}\kappa_i h$ in Eq. (23) can be expressed as $\lim_{h\to 0}\Sigma_{x=0}^{x=x_t}\kappa(x)h = \int_0^{x_t}\kappa(x)\mathrm{d}x$, and Φ_s in Eq. (27) can be written as

$$\lim_{h\to 0}\sum_{x=0}^{x=x_t-h}\frac{p(x + h)f(x + h)}{p^2(x + h) + \kappa^2(x + h)}$$

$$\times \frac{[\kappa(x)/f(x) - \kappa(x + h)/f(x + h)]}{h}h$$

$$= \int_0^{x_t}\frac{p(x)f(x)}{p^2(x) + \kappa^2(x)}\left|\frac{\mathrm{d}[\kappa(x)/f(x)]}{\mathrm{d}x}\right|\mathrm{d}x.$$

Similarly, Eq. (28) is expressed as

$$\lim_{h\to 0}\frac{p(x + h)/f(x + h) - p(x)/f(x)}{h} = \frac{p^2(x) + \kappa^2(x)}{f^2(x)},$$

and, furthermore, $\mathrm{d}[p(x)/f(x)]/\mathrm{d}x = [\kappa^2(x) + p^2(x)]/f^2(x)$.

Then Eq. (23) can be transformed into

$$\int_0^{x_t}\kappa(x)\mathrm{d}x + \int_0^{x_t}\frac{p(x)f(x)}{p^2(x) + \kappa^2(x)}\left|\frac{\mathrm{d}[\kappa(x)/f(x)]}{\mathrm{d}x}\right|\mathrm{d}x$$

$$= N\pi + \tan^{-1}\left(\frac{f_0}{f_c}\frac{p_c}{\kappa_0}\right) + \frac{\pi}{2} \qquad (N = 0,1,2,...), \tag{29}$$

where

$$\kappa(x)$$

$$= \begin{cases} \kappa^{\text{TM}}(x) = \dfrac{n_z(x)}{n_x(x)}[k_0^2 n_x^2(x) - \beta^2]^{1/2} & \text{for TM mode} \\[2mm] \kappa^{\text{TE}}(x) = [k_0^2 n_y^2(x) - \beta^2]^{1/2} & \text{for TE mode} \end{cases}.$$

$p(x)$ is determined by the following differential equation;

$$\frac{\mathrm{d}[p(x)/f(x)]}{\mathrm{d}x} = \frac{\kappa^2(x) + p^2(x)}{f^2(x)}, \qquad p(x_t) = p_t, \tag{30}$$

where

$$f(x) = \begin{cases} n_z^2(x) & \text{for TM mode} \\ 1 & \text{for TE mode} \end{cases}.$$

As the subscripts i and $i + 1$ indicate the neighboring segments of layers in the guiding region, shown in Eqs. (24) and (27), Φ_s is interpreted as phase contributions from the scattered subwaves.[20] If we set $\kappa_{i+1}/f_{i+1} = \kappa_i/f_i$, which exists in the step-index profile, $\Phi_s = 0$ will be obtained, consistent with the above analysis of the step-index case. Thus Eq. (29) shows a clear physical meaning: The two terms or the left-hand side present half of the phase contribution of the guiding waves and the subwaves, and the second and third terms on the right-hand side offer half of the phase loss at the interface and the turning point, respectively. When the sum of phase contributions and losses is equal to $2N\pi$, the optical wave will be guided and propagate in the waveguide.

For the situation when two turning points occur, as shown in Fig. 5, the dispersion equation can be straightforwardly presented, according to the above analysis, as

$$\int_{x_{t1}}^{x_{t2}} \kappa(x)\mathrm{d}x + \int_{x_{t1}}^{x_{t2}} \frac{p(x)f(x)}{p^2(x) + \kappa^2(x)} \left| \frac{\mathrm{d}[\kappa(x)/f(x)]}{\mathrm{d}x} \right| \mathrm{d}x$$

$$= (N + 1)\pi \qquad (N = 0,1,2,...). \quad (31)$$
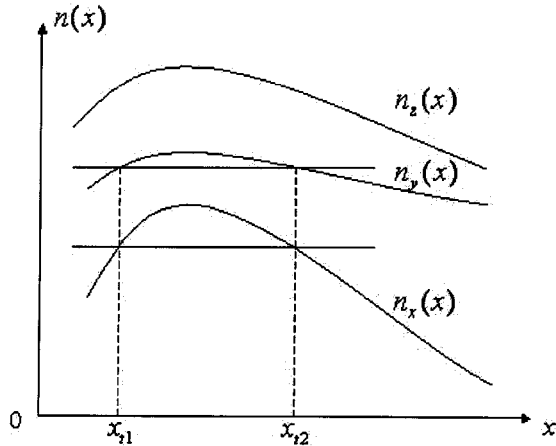
Fig. 5. Graded-index anisotropic waveguide with two turning points.

D. Discontinuation in a Graded Anisotropic Waveguide
A discontinuous index profile is also considered, as shown in Fig. 6. Figure 6(a) demonstrates a condition where a discontinuous point is situated in the oscillatory region, which provides an extra phase contribution, referred to as Φ_d. From Eqs. (24)–(26), we can find that, at a given point x,

$$p(x) = \kappa(x)\tan\left\{ \tan^{-1}\left[\frac{f(x)}{f(x + h)} \frac{p(x + h)}{\kappa(x)} \right] - \kappa(x)h \right\},$$
$$(32)$$

and the phase contribution of scattered subwaves of the neighboring layers on the left and the right of point x is

$$\Phi(x) = \tan^{-1}\left[\frac{p(x + h)}{\kappa(x + h)} \right] - \tan^{-1}\left[\frac{f(x)}{f(x + h)} \frac{p(x + h)}{\kappa(x)} \right].$$
$$(33)$$

When $h \to 0$, we obtain

$$p(x - 0) = \frac{f(x - 0)p(x + 0)}{f(x + 0)}, \quad (34)$$

$$\Phi(x) = \tan^{-1}\left[\frac{p(x + 0)}{\kappa(x + 0)} \right]$$
$$- \tan^{-1}\left[\frac{f(x - 0)}{f(x + 0)} \frac{p(x + 0)}{\kappa(x - 0)} \right]. \quad (35)$$

Then the extra inner phase contribution at the discontinuous point x_d can be calculated as

$$\Phi_d = \tan^{-1}\left[\frac{p^-(x_d)}{\kappa^-(x_d)} \right] - \tan^{-1}\left[\frac{f^+(x_d)}{f^-(x_d)} \frac{p^-(x_d)}{\kappa^+(x_d)} \right], \quad (36)$$

where

(a)   (b)

Fig. 6. Discontinuous index profile in a graded-index anisotropic waveguide.

$$\kappa^\pm(x_d) = \begin{cases} [\kappa^\pm(x_d)]^{TM} = \dfrac{n_z^\pm(x_d)}{n_x^\pm(x_d)}\{k_0^2[n_x^\pm(x_d)]^2 - \beta^2\}^{1/2} \\ \qquad\qquad\qquad\qquad\qquad\quad \text{for TM mode,} \\ [\kappa^\pm(x_d)]^{TE} = \{k_0^2[n_y^\pm(x_d)]^2 - \beta^2\}^{1/2} \\ \qquad\qquad\qquad\qquad\qquad\quad \text{for TE mode} \end{cases}$$

$$f^\pm(x_d) = \begin{cases} [n_z^\pm(x_d)]^2 & \text{for TM mode} \\ 1 & \text{for TE mode} \end{cases}.$$

Finally, just as for the continuous graded-index profile, the dispersion equation for the discontinuous distribution can be obtained:

$$\int_{x_{t1}}^{x_{t2}} \kappa(x)\mathrm{d}x + \int_{x_{t1}}^{x_d} \frac{p(x)f(x)}{p^2(x) + \kappa^2(x)} \left| \frac{\mathrm{d}[\kappa(x)/f(x)]}{\mathrm{d}x} \right| \mathrm{d}x$$

$$+ \int_{x_d}^{x_{t2}} \frac{p(x)f(x)}{p^2(x) + \kappa^2(x)} \left| \frac{\mathrm{d}[\kappa(x)/f(x)]}{\mathrm{d}x} \right| \mathrm{d}x$$

$$+ \Phi_d = (N + 1)\pi \quad (N = 0,1,2,...). \quad (37)$$

$p(x)$ is determined by the following differential equation:

$$\frac{\mathrm{d}[p(x)/f(x)]}{\mathrm{d}x} = \frac{\kappa^2(x) + p^2(x)}{f^2(x)},$$

$$p(x_t) = p_t,$$

$$p^+(x_d) = \frac{f^+(x_d)}{f^-(x_d)}p^-(x_d). \quad (38)$$

Another situation is depicted in Fig. 6(b), where the effective index is between $n^+(x_d)$ and $n^-(x_d)$. This situation can be solved very similarly to the continuous graded-index profile. However, in this case, half of the phase loss at the discontinuous point is $\tan^{-1}\{[f^+(x_d)/f^-(x_d)][p_t/\kappa^+(x_d)]\}$ instead of $\pi/2$, for $\kappa^+(x_d)$ is not equal to zero, which can be easily found from Eq. (22). Thus the dispersion equation for such a situation can be written as

$$\int_{x_{t1}}^{x_d} \kappa(x)\mathrm{d}x + \int_{x_{t1}}^{x_d} \frac{p(x)f(x)}{p^2(x) + \kappa^2(x)} \left| \frac{\mathrm{d}[\kappa(x)/f(x)]}{\mathrm{d}x} \right| \mathrm{d}x$$

$$= \left(N + \frac{1}{2}\right)\pi + \tan^{-1}\left[\frac{f^+(x_d)}{f^-(x_d)} \frac{p_t}{\kappa^+(x_d)}\right]$$

$$(N = 0,1,2,...). \quad (39)$$

$p(x)$ is determined by the following differential equation:

$$\frac{\mathrm{d}[p(x)/f(x)]}{\mathrm{d}x} = \frac{\kappa^2(x) + p^2(x)}{f^2(x)}, \qquad p^+(x_d) = \frac{f^+(x_d)}{f^-(x_d)}p_t \quad (40)$$

If the discontinuous point x_d is beyond the turning point, it can also be found that $p^+(x_d) = [f^+(x_d)/f^-(x_d)]p^-(x_d)$, which can be directly obtained evolved from Eqs. (21) by setting $h \to 0$.

It needs to be noted that Eqs. (29), (31), (37), and (39) are approximate, for we have neglected the second-order

Table 1. Comparison of Calculated Values of *b* for a Four-Layer Structure

TM Mode	Present Method	TMM	FD-BPM ($\Delta x = 3.9$ nm)	FD (W=5 μm, $\Delta x = 3.9$ nm)
TM_0	0.671163	0.671163	0.671158	0.671157
TM_1	0.100807	0.100810	—	0.100816

minor terms, that is, we consider just the phase contribution of the first-order scattered subwaves and the higher-order subwaves are ignored. This approximation is proved to be reasonable and reliable by various numerical approaches in Section 3.

3. NUMERICAL RESULTS

To verify the reliability of the current method, we consider diversified waveguide structures, as adopted in Refs. 15 and 16. To realize a practical numerical approach, the thickness of the divided layer presented in our analysis cannot be infinitely small, so a uniform thickness of 5 μm is introduced for all simulations. For a four-layer anisotropic waveguide, at a wavelength of 957.44 nm, the refractive index of each layer is given by $n_{0,x,y,z} = 1.4526$, $n_{1x} = 1.6721$, $n_{1y} = n_{1z} = 1.6738$, $n_{2x} = 1.5630$, $n_{2y} = n_{2z} = 1.5622$, and $n_{3x,y,z} = 1.0$, and the thicknesses of the first guiding layer, h_1, and the second guiding layer, h_2, are 591 and 600 nm, respectively. The calculated values of b, which is defined as $(N_{eff}^2 - n_{0x}^2)/(n_{1x}^2 - n_{0x}^2)$ for each TM mode, are shown in Table 1 together with the results calculated with the TMM, FD-BPM, and FD methods of Ref. 16. From the table, we can see that the results of the present method are almost the same as those of the other methods. In the numerical approach, we found that the TM_1 and TM_0 guided modes just cover the two situations in the analysis of the four-layer structure.

An annealed proton-exchanged (APE) waveguide in lithium niobate that has a graded-index profile is used as another example to testify to our theory. The proton-exchange process increases the extraordinary index in the guiding layer while decreasing the ordinary index; thus one can stimulate only TM modes in Z-cut samples and TE modes in X- and Y-cut substrates. After annealing, both the extraordinary and ordinary indices redistribute into a graded profile. Here we assume that the index distribution in an APE waveguide sample has the following form:

$$n_e(x) = \begin{cases} n_{se} + \Delta n_e \exp\left(-\dfrac{x^2}{D_1^2}\right), & x \geq 0 \\ n_{ce}, & x < 0 \end{cases},$$

$$n_o(x) = \begin{cases} n_{so} + \Delta n_o \exp\left(-\dfrac{x^2}{D_2^2}\right), & x \geq 0 \\ n_{co}, & x < 0 \end{cases}.$$

For a 632.8-nm He–Ne laser, $n_{se} = 2.2$, $n_{so} = 2.286$, $\Delta n_e = 0.01$, $\Delta n_o = -0.004$, $n_{ce} = n_{co} = 1.0$, and $D_1 = D_2 = 5\ \mu$m. Comparisons of the effective index N_{eff} calculated with the present method and with the other methods of Ref. 16 are shown in Table 2. It is easily found that the values calculated with the present method have a very good accuracy.

To further verify the universal applicability of the method, we introduce a complicated discontinuous refractive-index profile in a Ti-diffused proton-exchanged (TIPE) LiNbO$_3$ waveguide with SiO$_2$ buffer and air cover. At the wavelength of 632.8 nm, the index profile of the TIPE + SiO$_2$ waveguide sample is given by

$$n_e(x)$$

$$= \begin{cases} n_c, & x \leqslant -1 \\ n_b, & -1 < x \leqslant 0 \\ n_{es} + 0.014\exp(-x^2/3^2) + 0.11, & 0 < x \leqslant 1 \\ n_{es} + 0.014\exp(-x^2/3^2), & x > 1 \end{cases},$$

$$n_o(x)$$

$$= \begin{cases} n_c, & x \leqslant -1 \\ n_b, & -1 < x \leqslant 0 \\ n_{os} + 0.009\exp(-x^2/3^2) - 0.04, & 0 < x \leqslant 1 \\ n_{os} + 0.009\exp(-x^2/3^2), & x > 1 \end{cases},$$

where $n_{es} = 2.2$, $n_{os} = 2.286$, $n_b = 1.45$, and $n_c = 1.0$. To reliably cope with the discontinuous profile in the above theory, we need to make some prior assumptions on the effective index: above the discontinuous segment, in the discontinuous segment, and under the discontinuous segment. Each assumption should be implemented with the corresponding dispersion equation to cover all potential stimulated modes. For an X-cut, Y-propagating sample, the results of TE modes calculated by the current method and the other methods of Ref. 16 are demonstrated in Table 3. As shown in the table, the current analytical method agrees quite well with the accurate numerical schemes.

We finally analyze a symmetric discontinuous anisotropic waveguide with $n_x(x) = 1.65[1 - 0.115(x/d)^2]^{1/2}$, $n_y(x) = n_z(x) = 1.48[1 - 0.0135(x/d)^2]^{1/2}$, and $n_c = n_s = 1.46$, where $-d \leqslant x \leqslant d$. TM modes of the waveguide are calculated at 860 nm. Just as in the last cal-

Table 2. Calculated Results of Effective Index N_{eff} for an Anisotropic Graded-Index Profile

Waveguide Anisotropy	Mode	Present Method	TMM (2000 layers)	FD ($W = 25\ \mu$m, 500 grids)
Z-cut,	TM$_0$	2.207390	2.207393	2.207394
Y-propagation,	TM$_1$	2.204371	2.204374	2.204376
APE-LiNbO$_3$	TM$_2$	2.201986	2.201988	2.201990
	TM$_3$	2.200390	2.200390	2.200392
X-cut,	TE$_0$	2.207359	2.207362	2.207363
Y-propagation,	TE$_1$	2.204272	2.204274	2.204277
APE-LiNbO$_3$	TE$_2$	2.201850	2.201851	2.201854
	TE$_3$	2.200284	2.200284	2.200286

Table 3. Calculated Values of Effective Index N_{eff} for an Anisotropic TIPE LiNbO$_3$ Waveguide with Discontinuous Profile

TE Mode	Present Method	TMM (3000 layers)	FD ($W = 15\ \mu$m, $\Delta x = 10$ nm)
TE$_0$	2.30851	2.30851	2.30851
TE$_1$	2.26436	2.26436	2.26437
TE$_2$	2.20703	2.20704	2.20705
TE$_3$	2.20220	2.20221	2.20222
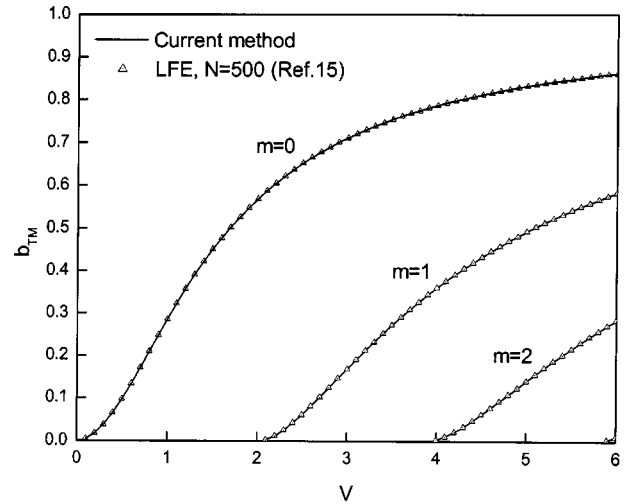
Fig. 7. Normalized mode index $b_{\text{TM}} = (\beta^2 - k_0^2 n_c^2)/(k_0^2 n_{x,\max}^2 - k_0^2 n_c^2)$ with normalized frequency $V = k_0 d(n_{x,\max}^2 - n_c^2)^{1/2}$ of TM modes in a symmetric anisotropic waveguide.

culation, the propagation constants in the discontinuous distribution are presupposed for diversified situations, and every condition is considered. The simulated results of a normalized mode index $b_{\text{TM}} = (\beta^2 - k_0^2 n_c^2)/(k_0^2 n_{x,\max}^2 - k_0^2 n_c^2)$ with a normalized frequency $V = k_0 d(n_{x,\max}^2 - n_c^2)^{1/2}$, in comparison with the Lanczos–Fourier expansion (LFE) technique,[15] are demonstrated in Fig. 7. It can be found that the current analytical method is also in good agreement with the accurate numerical approach.

4. CONCLUSIONS

In summary, a compact method based on an analytical transfer-matrix method and an improved EAV assumption is suggested to analyze an anisotropic planar waveguide. The eigenvalue equations are proposed by the method for both TM and TE modes in explicit and analytical forms. A multilayer structure, graded-index distributions with one and two turning points, and discontinuous profiles are separately investigated. It is shown by examples that this method can obtain accurate results compared with numerical methods, while it holds considerable physical insight. The proposed phase contribution of scattered subwaves and phase contribution at a discontinuous point may serve to reliably model and design complicated anisotropic waveguide configurations.

ACKNOWLEDGMENTS

REFERENCES

1. D. P. Gia Russo and J. H. Harris, "Wave propagation in anisotropic thin film optical waveguides," J. Opt. Soc. Am. **63**, 138–145 (1973).
2. J. Ctyroky and M. Cada, "Generalized WKB method for the analysis of light propagation in inhomogeneous anisotropic optical waveguides," IEEE J. Quantum Electron. **QE-17**, 1064–1070 (1981).
3. P. Yeh, "Optics of anisotropic layered media: a new 4 × 4 matrix algebra," Surf. Sci. **96**, 41–53 (1980).
4. S. Visnovsky, "Magnetic-optic effects in ultrathin structures at longitudinal and polar magnetizations," Czech. J. Phys. **48**, 1083–1104 (1998).
5. E. A. Kolosovsky, D. V. Petrov, A. V. Tsarev, and I. B. Yakovkin, "An exact method for analyzing light propagation in anisotropic inhomogeneous optical waveguides," Opt. Commun. **43**, 21–25 (1982).
6. L. M. Walpita, "Solutions for planar optical waveguide equations by selecting zero elements in a characteristic matrix," J. Opt. Soc. Am. A **2**, 595–602 (1985).
7. L. Tsang and S. L. Chuang, "Improved coupled-mode theory for reciprocal anisotropic waveguide," J. Lightwave Technol. **6**, 304–311 (1988).
8. G. Tartarini, P. Bassi, S. F. Chen, M. P. De Micheli, and D. B. Ostrowsky, "Calculation of hybrid modes in uniaxial planar optical waveguides: application to proton exchanged lithium niobate waveguides," Opt. Commun. **101**, 424–431 (1993).
9. L. Nuno, J. V. Balbastre, and H. Castane, "Analysis of general lossy inhomogeneous and anisotropic waveguides by the finite-element method (FEM) using edge elements," IEEE Trans. Microwave Theory Tech. **45**, 446–449 (1997).
10. S. Selleri, L. Vincetti, A. Cucinotta, and M. Zoboli, "Complex FEM modal solver of optical waveguides with PML boundary conditions," Opt. Quantum Electron. **33**, 359–371 (2001).
11. I. Bardi and O. Biro, "An efficient finite-element formulation without spurious modes for anisotropic waveguides," IEEE Trans. Microwave Theory Tech. **39**, 1133–1139 (1991).
12. M. Koshiba, K. Hayata, and M. Suzuki, "Finite-element formulation in terms of the electric-field vector for electromagnetic waveguide problems," IEEE Trans. Microwave Theory Tech. **MTT-33**, 900–905 (1985).
13. V. Schulz, "Adjoint high-order vectorial finite elements for nonsymmetric transversally anisotropic waveguides," IEEE Trans. Microwave Theory Tech. **51**, 1086–1095 (2003).
14. S. G. Garcia, T. M. Hung-Bao, R. G. Martin, and B. G. Olmedo, "On the application of finite methods in time domain to anisotropic dielectric waveguides," IEEE Trans. Microwave Theory Tech. **44**, 2195–2206 (1996).
15. P. A. Koukoutsaki, I. G. Tigelis, and A. B. Manenkov, "Guided-mode analysis by the Lanczos–Fourier expansion," J. Opt. Soc. Am. A **19**, 2293–2300 (2002).
16. H. P. Uranus, H. J. W. M. Hoekstra, and E. Vangroesen, "Finite difference scheme for planar waveguides with arbitrary index profiles and its implementation for anisotropic waveguides with a diagonal permittivity tensor," Opt. Quantum Electron. **35**, 407–427 (2003).
17. S. Gaal, "Surface integral method to determine guided modes in uniaxially anisotropic embedded waveguides," Opt. Quantum Electron. **31**, 763–780 (1999).
18. L. Zhan and Z. Cao, "Exact dispersion equation of a graded refractive-index optical waveguide based on the equivalent attenuated vector," J. Opt. Soc. Am. A **15**, 713–716 (1998).
19. Z. Cao, Y. Jiang, Q. S. Shen, X. M. Dou, and Y. L. Chen, "Exact analytical method for planar optical waveguides with arbitrary index profile," J. Opt. Soc. Am. A **16**, 2209–2212 (1999).
20. Z. Cao, Q. Liu, Q. S. Shen, X. M. Dou, and Y. L. Chen, "Quantization scheme for arbitrary one-dimensional potential wells," Phys. Rev. A **63**, 054103 (2001).